Tunnel Fire Simulation Model with Multi-Layer Zone Concept

KEICHI SUZUKI[1], TAKEYOSHI TANAKA[2] and KAZUNORI HARADA[3]
[1] Institute of Technology, Shimizu Construction Corporation
3-4-17 Echujima Koto-ku, Tokyo 135-8530, Japan
[2] Disaster Prevention Research Institute, Kyoto University
Gokasho, Uji, Kyoto 611-0011, Japan
[3] Department of Architecture and Architectual Engineering, Graduate School of Eng., Kyoto University, Katsura Campus C2-406, Nishikyo-ku, Kyoto 615-8540, Japan

ABSTRACT

In this study, a new zone modeling approach, called a Multi Layer Zone (MLZ) model was extended to adapt to predict smoke movement in a tunnel fire, including vertical distributions of temperature and chemical species concentrations. In this model the volume of a tunnel is divided into multiple of areas and each of then is further divided into multiple horizontal layers as the control volumes. The physical properties, such as temperature and species concentrations, in each layer of each area are assumed to be uniform. The boundary walls are also divided into segments at uniform temperature in accordance with the layer division. Radiation heat transfer between the layers and between the layers and the wall segments is calculated, as well as the convective heat transfer between the layers and the wall segments. Air entrainment into the fire plume and the flame, considering the effect of the horizontal flow around it, is calculated with a simple set of equations. This model still retains the advantage of zone models in terms of computational load, hence it is expected to be useful for practical applications associated with fire safety design of tunnels. For calibration and verification of the model, comparisons of the predictions by the present model are presented against measurements in two cases of experiments using a tunnel facility (*Length* 28m) and predictions by FDS for the same test conditions. The predicted temperatures and velocities generally show satisfactory agreement with the experimental data.

KEYWORDS: tunnel fire, multi-layer zone model, smoke movement

NOMENCLATURE LISTING

A_f	area of floor (m^2)	Q_{radl}	radiation heat gain of layer (kW)
A_w	area of wall (m^2)	Q_{radw}	radiation heat transfer to wall (kW)
C_e	coefficient of entrainment	S	stoichiometric ratio air to fuel
C_p	specific heat of gas (kJ/kgK)	t	time (s)
C_w	specific heat of wall (kJ/kgK)	T	gas temperature (K)
d	hydraulic diameter of tunnel (m)	T_W	wall temperature (K)
d_f	diameter of fire source (m)	u	horizontal velocity (m/s)
F_b	buoyancy force	U_j	horizontal flow velocity (m/s)
F_f	friction force	V	volume of layer (m^3)
F_r	Froude number	W^*	buoyancy flow velocity from fire source
F_{LL}	View factor from layer to layer	x	depth from wall surface (m)
F_{WL}	View factor from layer to wall	Δx	length of area (m)
F_{LW}	View factor from wall to layer	Y	mass fraction of the species (kg/kg)
F_{FW}	View factor from wall to flame	Z	height from fire source (m)
g	gravity acceleration (m/s^2)	Z_v	height of virtual source origin (m)
h_h	horizontal enthalpy flow rate (kW)	Δz	depth of layer (m)

FIRE SAFETY SCIENCE–PROCEEDINGS OF THE NINTH INTERNATIONAL SYMPOSIUM, pp. 713-724
 / DOI:10.3801/IAFSS.FSS.9-713

h_v	vertical enthalpy flow rate (kW)	**Greek letters**	
k_w	thermal conductivity of wall (kW/mK)	α_c	convective heat transfer coefficient (kW/Km$_2$)
m	mass loss from the fuel (kg)	α_r	radiation absorptivity of layer
m_{ent}	mass flow rate into fire plume (kg/s)	α_{rw}	radiation absorptivity of wall
m_{fp}	mass flow rate into fire plume (kg/s)	χ_A	efficiency of combustion
m_v	vertical mass flow rate (kg/s)	Γ	mass production rate of fire (kg/s)
m_h	horizontal mass flow rate (kg/s)	λ	coefficient of friction
M_{fp}	mass fraction into fire plume (kg/s)	ρ	density of gas (kg/m^3)
M_v	vertical mass fraction rate (kg/s)	ρ_w	density of wall (kg/m^3)
M_h	horizontal mass fraction rate (kg/s)	σ	Stefan-Boltzmann coefficient
p	pressure difference (Pa)	**subscripts**	
p_v	dynamic pressure (Pa)	f	area number with fire
q_{ru}	upward heat flux (kW/m^2)	i	area number
q_{rd}	downward heat flux (kW/m^2)	ix	maximum number of areas
q_{rw}	horizontal heat flux (kW/m^2)	j	number of layers
Q_c	convective heat release rate (kW)	jx	maximum layer number
Q_r	radiation heat gain of layer (kW)	k	number of layers in the wall
Q_w	convection heat transfer to wall(kW)	l	gas species number
Q_{rad}	radiation heat release rate of fire(kW)	nb	neighboring area of i-th layer
Q_{radf}	radiation heat from flame(kW)	0	layer of floor lever

INTRODUCTION

Recently, computational fluid dynamics (CFD) models have been applied to some major tunnels for designing fire protection and smoke control systems [1]. CFD models can calculate the temperature and velocity field and predict the smoke movement due to a fire, throughout the domain of interest. Three-dimensional time-dependent equations based on the laws of fluid dynamics are solved numerically with the boundary conditions specific to the problem. An advantage of CFD models is that they can predict detailed

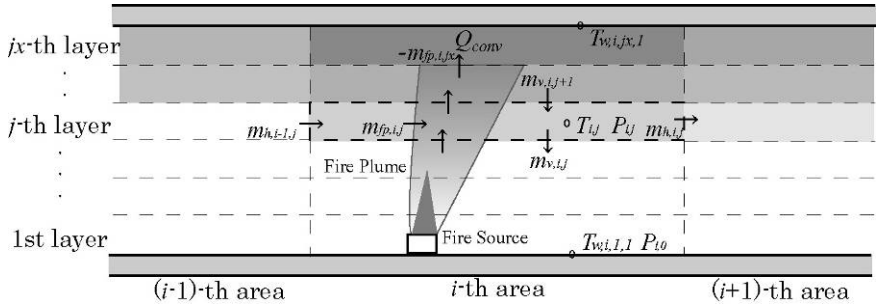

Fig. 1. The image of MLZ model to a tunnel fire

distributions of temperatures and velocities in the domain of interest. On the other hand, CFD models need long CPU time. It can often take more than a couple of days of computer time for only 1 minute of simulation time.

The other methods available for predicting smoke movement are zone models, which are used frequently for building fire safety design. Zone models assume that a compartment consists of one, two or three layers. The physical properties of each layer, such as gas temperature and species concentrations are assumed uniform. In the case of the two-layer zone models, the interface of the layers changes in height according to the mass inputs through a fire plume and heat transfer [2]. In a tunnel fire experiment, while a stratified layer situation can be observed, the layer interface is not always clear and the temperature varies rather gradually with height and distance from the fire origin. However, FASIT, which was a three-layer zone model to predict the smoke movement in tunnels, can calculate gas conditions in each uniform layer, including smoke and air mixing layers. Vertical temperature profiles can be roughly predicted within a practical computation time [3].

In this study, a new zone modeling approach, which we call a multi-layer zone model (MLZ model) [4], was extended to adapt prediction of smoke movement in tunnel fires, including vertical distributions of temperature and chemical species concentrations. In this model the volume of a tunnel is divided into a number of areas consisting of multiple horizontal layers as illustrated in Fig.1. The physical properties, such as the temperature and the species concentrations, in each layer are assumed to be uniform. The boundary walls are also divided into segments in accordance with the layer division. Radiation heat transfer between the fire source and the walls and between the layers and the wall segments are calculated as well as the convective heat transfer between the layers and the wall segments. Air entrainment into a fire plume and a flame, considered the effect of the horizontal flow around it, is calculated with the equations considering the influences of horizontal flow around them. This model still retains the advantage of zone models in terms of computational time so is expected to be useful for practical applications associated with fire safety design of tunnels.

THE MODEL

Governing Equations for Zone Properties

The principal equations for gas temperature of the MLZ model, called zone governing equations, are derived from the conservation equations for mass and internal energy and equation of state in each layer, as follows:

$$\frac{dT_{i,j}}{dt} = \frac{1}{C_p \rho_{i,j} V_{i,j}} \left[\left(C_p m_{fp,i,j} T_{i,j} - h_{fp,i,j} \right) + \sum_{nb} \left(C_p m_{h,nb \to i,j} T_{i,j} - h_{h,nb \to i,j} \right) \right.$$
$$\left. - \left(C_p m_{v,i,j+1} T_{i,j} - h_{v,i,j+1} \right) + \left(C_p m_{v,i,j} T_{i,j} - h_{h,i,j} \right) + Q_{w,i,j} + Q_{r,i,j} + Q_c \right] \quad (1)$$

where Q_c, the convective heat release rate from the fire source, exists in only *jx*-th layer (top layer) of the area with the fire. $m_{fp,i,j}$ is the mass flow rate entrained into the fire plume from the *j*-th layer of the i-th area (if *i* is not the area number with fire, $m_{fp,i,j}$ is 0). If $m_{v,i,j}$, the mass flow rate from the *j*-th layer to the (*j*-1)-th through the surface, is positive, the net flow through the interface of the (*j*+1)-th and the *i*-th layers is downward, otherwise upward. Then $h_{v,i,j}$, the horizontal enthalpy flow rate, deals with the change of the direction of the flow as follows:

$$h_{v,i,j} = \begin{cases} C_p m_{v,i,j} T_{i,j} & \left(m_{v,i,j} \geq 0 \right) \\ C_p m_{v,i,j} T_{i,j-1} & \left(m_{v,i,j} < 0 \right) \end{cases} \quad (2)$$

Likewise, the zone governing equation for mass fraction of species *l* in each layer is derived from the conservation equations for mass and gas species fraction and the equation of states in each laminated layer, as follows:

$$\frac{dY_{l,i,j}}{dt} = \frac{1}{\rho_{i,j} V_{i,j}} \Big[\left(m_{fp,j} Y_{l,i,j} - M_{fp,l,j} \right) + \sum_{nb} \left(m_{h,nb \to i,j} Y_{l,i,j} - M_{h,l,nb \to i,j} \right) - \left(m_{v,i,j+1} Y_{i,j} - M_{v,l,i,j+1} \right) + \left(m_{v,i,j} Y_{l,i,j} - M_{v,l,i,j} \right) + \Gamma \Big] \tag{3}$$

where $Y_{l,i,j}$ is the mass fraction of the species l in the j-th layer of the i-th area, Γ is the mass production rate of the species l by the fire source. In this model, the generation and consumption of the chemical species Γ (l: soot, O_2, CO_2, H_2O, N_2) per unit fuel consumed in combustion is calculated by assuming complete combustion. $M_{v,l,i,j}$ deals with the change of direction of the flow as follows:

$$M_{v,l,i,j} = \begin{cases} m_{v,i,j} Y_{l,i,j} & \left(m_{v,i,j} \geq 0 \right) \\ m_{v,i,j} Y_{l,i,j-1} & \left(m_{v,i,j} < 0 \right) \end{cases} \tag{4}$$

Mass Transport

To solve Eq.1 and 3, the rate terms in them must be formulated based on the relevant modeling of component processes of fire. This section deals with the modeling of the mass flow rates involved.

Mass flow rate through vertical boundaries

Adding the energy conservation equations of all layers and the equation of state, we have the mass conservation equations of each area at each time step, as follows:

$$\sum_{nb} \sum_{j} C_p m_{h,nb \to i,j} T_{nb,j} - \sum_{nb} \sum_{j} C_p m_{h,i \to nb,j} T_{i,j} + \sum_{j=1}^{jx} Q_{w,i,j} + \sum_{j=1}^{jx} Q_{r,i,j} + Q_c = 0 \tag{5}$$

The pressure differences, $p_{i,j}$, are computed simply (not like CFD) from the pressure difference at the standard level, $p_{i,0}$, and gravity as

$$p_{i,j} = p_{i,0} - g \sum_{k=1}^{j} \rho_{i,k} \Delta z \tag{6}$$

Then the velocities of horizontal flow through the boundary from the i-th layer to the (i+1)-th layer, $u_{i+1,j}$, are computed by Eq.7, which is obtained by arranging the equation of Bernoulli.

$$u_{i+1,j} = \begin{cases} \sqrt{\dfrac{2\left(p_{i,j} - p_{i+1,j} + p_v - F_f - F_b \right)}{\rho_{i,j}}} & \left(p_{i,j} - p_{i+1,j} + p_v - F_f - F_b \geq 0 \right) \\ -\sqrt{\dfrac{-2\left(p_{i,j} - p_{i+1,j} + p_v - F_f - F_b \right)}{\rho_{i,j}}} & \left(p_{i,j} - p_{i+1,j} + p_v - F_f - F_b < 0 \right) \end{cases} \tag{7}$$

$m_{h,i\text{-}i+1,j}$ and $m_{h,i+1\text{-}i,j}$ is shown by,

$$m_{h,i \to i+1,j} = \begin{cases} b \Delta z u_{i,j} \rho_{i,j} & \left(u_{i,j} \geq 0 \right) \\ 0 & \left(u_{i,j} < 0 \right) \end{cases} \tag{8}$$

$$m_{h,i+1\to i,j}=\begin{cases}0 & \left(u_{i,j}\ge 0\right)\\ b\Delta z u_{i,j}\rho_{i+1} & \left(u_{i,j}<0\right)\end{cases} \tag{9}$$

where u, m_h and p are calculated iteratively by the Gauss-Seidel method. Firstly temporal u, m_h and p are computed in each area, using Newton-Raphson method with Eq.5. Then this cycle is iterated until all *ps* become almost steady (within 10^{-6} Pa). The dynamic pressure, p_v, is calculated from the higher velocity of both adjacent boundaries as follows,

$$p_v=\begin{cases}\frac{1}{2}\rho_{i,j}u_{i,j}^2 & \left(\left|\max\left(u_{i,j},0\right)\right|\ge\left|\min\left(u_{i+2,j},0\right)\right|\right)\\ \frac{1}{2}\rho_{i+1,j}u_{i+2,j}^2 & \left(\left|\max\left(u_{i,j},0\right)\right|<\left|\min\left(u_{i+2,j},0\right)\right|\right)\end{cases} \tag{10}$$

F_b is the buoyancy force in the case of tunnel with leaning axis and F_f, the friction with the walls, the ceilings and the floors, becomes

$$F_f=\frac{\lambda}{2d}\rho_{i,j}\Delta x u_{i,j}\left|u_{i,j}\right|\frac{A_{w,i,j}}{\sum_{j=1}^{jx}A_{w,i,j}} \tag{11}$$

Mass flow rate entrained into fire plume

The gas entrainment into the fire plume is important in smoke movement predictions. The mass flow rate in the fire plume in the windless condition at Z, $m_{ent}(Z)$, is assumed to be given by the following equation by Delichatsios and Orloff [5]

$$\frac{m_{ent}(Z)\mathrm{Fr}}{\left(\chi_A S+1\right)m}=0.086\left(Z/d_f\right)^{1/2}\quad Z/d_f<1.0 \tag{12a}$$

$$\frac{m_{ent}(Z)\mathrm{Fr}}{\left(\chi_A S+1\right)m}=0.093\left(Z/d_f\right)^{3/2}\quad 1.0<Z/d_f<4.0 \tag{12b}$$

$$\frac{m_{ent}(Z)\mathrm{Fr}}{\left(\chi_A S+1\right)m}=0.018\left(Z/d_f\right)^{5/2}\quad Z/d_f>4.0 \tag{12c}$$

$$\frac{m_{ent}(Z)\mathrm{Fr}}{\left(\chi_A S+1\right)m}=0.21\mathrm{Fr}^{1/3}\left\{\left(Z+Z_v\right)/d_f\right\}^{5/3}\quad Z>\textit{flame height} \tag{12d}$$

where Fr is the Froude number, χ_A is the efficiency of combustion (default 1), S is the stoichiometric ratio air to fuel (default 15, for general oil fuels), m is the mass loss from the fuel, Z is the height from the fire source, Z_v is the virtual source origin based on entrainment and d_f is the diameter of the fire source. In this model, gas entrainment from j-th layer, $m_{fp,i,j}$, is gained by using $m_{ent}(j\Delta z)$ and $m_{ent}((j-1)\Delta z)$ at the height of upper and lower boundaries as

$$m_{fp,i,j}=C_e\left\{m_{ent}\left(j\Delta z\right)-m_{ent}\left(\left(j-1\right)\Delta z\right)\right\} \tag{13}$$

where C_e is the entrainment coefficient, increasing by the horizontal flow around the fire plume. The relation is shown as Fig.2 in the experiment [6] and set to the thick line in this model as follows

$$C_e = \begin{cases} 3 & \left(12U_j/W^* \geq 3\right) \\ 12U_j/W^* & \left(1 < 12U_j/W^* < 3\right) \\ 1 & \left(12U_j/W^* \leq 1\right) \end{cases} \quad (14) \qquad (14)$$

where U_j / W^* is the non-dimensional horizontal flow velocity in the *j*-th layer of the *i*-th area, U_j, is the horizontal flow velocity around the plume and *W** is the buoyancy flow velocity from the fire source, $\left(=\frac{Q_c g}{b\rho_\infty T_\infty C_p}\right)$. At *jx*-layer, the gas is emitted from the fire plume, hence $m_{fp,i,jx}$ becomes

$$m_{fp,i,jx} = -\sum_{j=1}^{jx-1} m_{fp,i,j} \qquad (15)$$

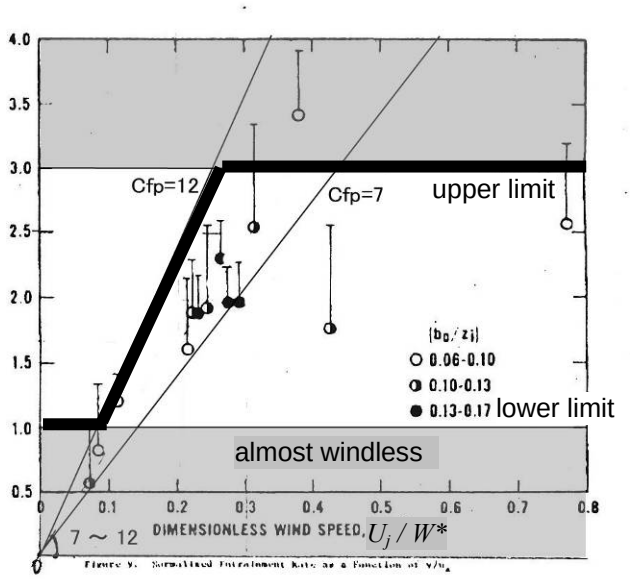

Fig. 2. The entrainment coefficient of the fire plume [6]

Mass flow rate through horizontal surfaces of layers

The mass flow rate through horizontal openings, $m_{v,i,j}$ is calculated by the equation of mass conservation in the *j*-th layer by substituting the mass flow rate through the upper surface

$$m_{v,i,j} = \begin{cases} \dfrac{h_{v,i,j}}{C_p T_{i,j}} & \left(h_{v,i,j} \geq 0\right) \\ \dfrac{h_{v,i,j}}{C_p T_{i,j-1}} & \left(h_{v,i,j} < 0\right) \end{cases} \qquad (16)$$

Where:

$$h_{v,i,j} = -h_{fp,i,j} + \sum_{nb} h_{h,nb\to i,j} - \sum_{nb} h_{h,i\to nb,j} + h_{v,i,j+1} + Q_{w,i,j} + Q_{r,i,j} \qquad (17)$$

Heat Transfer

Radiation heat transfer

In the model, the radiation heat flux is assumed to consist of three directional components between layers or layer and wall, i.e. the upward, the downward and the horizontal one from each layer as shown by arrows in Fig.3. The upward, downward and horizontal heat fluxes, $q_{ru,i,j}$, $q_{rd,i,j}$ and $q_{rw,i,j}$ are calculated as follows;

$$q_{ru,i,j} = \left(1-\alpha_{r,i,j}\right) F_{LL,i,j} q_{ru,i,j-1} + \alpha_{r,i,j}\sigma T_{i,j}^4 + \left(1-\alpha_{r,i,j}\right) F_{WL,i,j}\{(1-\alpha_{rw,i,j}) q_{rw,i,j} + \alpha_{rw,i,j}\sigma T_{w,i,j,1}^4\} \qquad (18)$$

$$q_{rd,i,j} = \left(1-\alpha_{r,i,j}\right) F_{LL,i,j} q_{rd,i+1,j} + \alpha_{r,i,j}\sigma T_{i,j}^4 + \left(1-\alpha_{r,i,j}\right) F_{WL,i,j}\{(1-\alpha_{rw,i,j}) q_{rw,i,j} + \alpha_{rw,i,j}\sigma T_{w,i,j,1}^4\} \qquad (19)$$

$$q_{rw,i,j} = \left(1-\alpha_{r,i,j}\right) F_{LW,i,j} q_{ru,i,j-1} + \left(1-\alpha_{r,i,j}\right) F_{LW,i,j} q_{rd,i,j+1} + \alpha_{r,i,j}\sigma T_{w,i,j,1}^4 + Q_{radw,j} \Big/ A_{w,i,j} \quad (20)$$

where $\alpha_{r,i,j}$ the radiation absorptivity, changes according to the gas temperature and mass fractions of CO_2, H_2O and soot, whose spectra are not uniform. In this model, the Fortran program ABSORB, developed by Modak [7], is used to calculate the radiation absorptivity.

In the fire room, radiation heat transfer from the flame (a point at the mean flame height, assumed *jm*-th) to the wall segments is considered, as shown by broken lines in Fig. 3. The fraction of radiation heat from the flame point to the surface of the *j*-th wall segment, $Q_{radf,i,j}$, is given

$$Q_{radf,i,j} = Q_{rad} F_{FW,i,j} \quad (21)$$

where $F_{FW,i,j}$ is the view factor from the flame point to the *j*-th wall. $Q_{radf,i,j}$ is partially absorbed in the layers before reaching the *j*-th wall. The rate of the radiation heat reached to *j*-th wall, $Q_{radw,i,j}$, is calculated by

$$Q_{radw,i,j} = \left(1-\alpha_{r,i,j}\right)\left(1-\alpha_{r,i,j-1}\right)\cdots\left(1-\alpha_{r,i,jm}\right) Q_{radf,i,j} \quad (22)$$

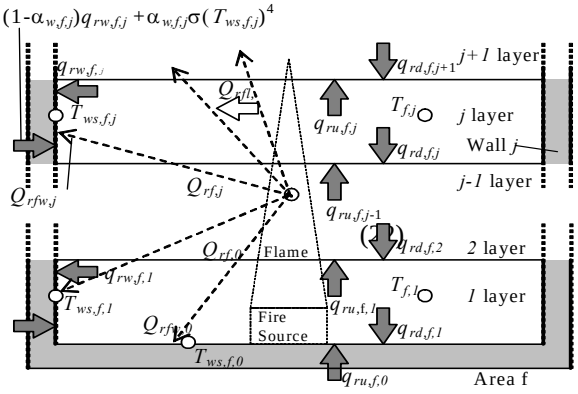

Fig. 3. Radiation heat transfer with fire

The rate of radiation absorbed in the *j*-th layer from the flame point $Q_{radl,i,j}$ becomes

$$Q_{radl,j} = \sum_{k=j}^{jx+1} \alpha_{r,j}\left(1-\alpha_{r,j-1}\right)\cdots\left(1-\alpha_{r,jm}\right) Q_{radf,k} \quad (23)$$

Hence the net radiation heat gain of the layer, $Q_{r,i,j}$, is

$$\begin{aligned} Q_{r,i,j} &= A_{f,i}\left(q_{ru,i,j-1} - q_{ru,i,j} + q_{rd,i,j+1} - q_{rd,i,j}\right) \\ &\quad - A_{w,i,j}\left[q_{rw,i,j-1} - \left\{\left(1-\alpha_{rw,i,j}\right)q_{rw,i,j} + \alpha_{rw,i,j}\sigma T_{W,i,j,1}^4\right\}\right] + Q_{radl,i,j} \end{aligned} \quad \text{(if } i \neq f,\ Q_{radl,i,j} = 0\text{)} \quad (24)$$

Convection heat transfer

The rate of convection heat transfer to the wall boundary, $Q_{w,i,j}$, is calculated as follows:

$$Q_{w,i,j} = \alpha_{c,i,j}\left(T_{i,j} - T_{W,i,j,1}\right) A_{w,i,j} + A_{w,i,j}\left[q_{rw,i,j} - \{(1-\alpha_{rw,i,j})q_{rw,i,j} + \alpha_{rw,i,j}\sigma T_{W,i,j,1}^4\}\right] \quad (25)$$

where $\alpha_{c,i,j}$, the heat transfer coefficient of the wall, is added with α_{c1}, the efficiency of flow by Jurges, and α_{c2}, temperature of the layer by Tanaka etc. [2] as

$$\alpha_{C1} = 0.0058 + 3.9u_{i,j} \quad (26)$$

$$\alpha_{C2} = \begin{cases} 0.005 & \left(\overline{T}_{i,j} \le 300\right) \\ 0.001\left(0.02\overline{T}_{i,j} - 1\right) & \left(300 < \overline{T}_{i,j} \le 800\right) \\ 0.015 & \left(\overline{T}_{i,j} > 800\right) \end{cases} \quad (27)$$

$$\alpha_{C,i,j} = \left(\alpha_{C1} - 0.005\right) + \alpha_{C2} \quad (28)$$

where $\overline{T}_{i,j}$ is the average of gas and wall temperature ($\overline{T}_{i,j} = (T_{i,j} + T_{w,i,j,1})/2$).

Conduction heat transfer

Conduction heat transfer in the wall is calculated by TDMA method implicitly using the one-dimensional differential equation of Eq. (29). The image of the temperature profile is shown as Fig. 4.

$$\frac{\partial T_{W,i,j}}{\partial t} = \frac{k_w}{\rho_w C_w} \frac{\partial^2 T_{W,i,j}}{\partial x^2} \quad (29)$$

From the above formula, $T_{w,i,j,k}$, the temperature of the wall at the k-th mesh from the surface mesh, can be solved. $T_{w,i,j,1}$ is the temperature of the wall surface. The boundary conditions are as follows:

$$k_W \left.\frac{\partial T_{W,i,j,1}}{\partial x}\right|_{x=0} = Q_{w,i,j} / A_{w,i,j}$$

$$T_{W,i,j,kx} = T^0_{W,i,j,kx} \quad (const.)$$

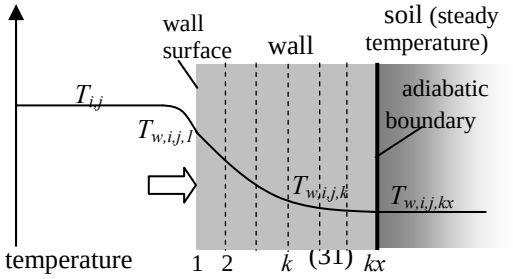

Fig. 4. The image of wall temperature calculation

The depth to the virtual adiabatic boundary must be predetermined for the calculation, however in most cases of tunnel fire prediction it is enough to select the depth of the concrete wall.

COMPARISON WITH EXPERIMENTAL RESULTS

Experimental Conditions

In this section, the temperature and velocity data from 2 fire experiments in a rectangular piped facility are compared with the predictions of the model for validation. The height and width of the facility were 1.79m and the length was 27.88m. The outline and measuring points are shown in Fig.5. Fig.6 shows the inside of the facility. One side of the wall and the floor was lined with plywood board, the ceiling and the other side of the wall were covered by insulation board. Both ends were opened, however they were covered loosely by sheets to prevent the influence of outdoor wind. The vertical distributions of temperature in 14 lines were measured by thermocouples of type-T (diameter was 0.65mm), and the horizontal wind velocity distributions in 4 lines were measured by hot wire anemometers (the limited temperature was 60°C). The fuel used was methanol in a circular pan with a diameter of 0.5m. The total heat release rate had been measured to be 55 kW buying a cone calorimeter before this experiment. The fuel pan was placed in another container where water was put for preventing temperature rise of the fuel. Therefore an almost constant heat release rate was kept. In case 1 the condition was natural ventilation without fans. In case 2, two fans (outside diameter was about 0.3m) were installed and adjusted to flow with 0.5 m/s average wind.

The detailed distribution of velocity in the facility was measured without the fire, the velocities were within 0.3-0.7m/s. In the experiment, the density of the gas, carbon dioxide concentration etc. were not measured.

Calculation Conditions

The conditions of the calculations using the MLZ model, such as the geometry of the volume, the initial and outside air temperature, the opening and the wall boundaries in the domain and the heat release rate were determined according to the experimental conditions. The volume in the domain was divided into 15 areas and 9 layers equally (layer size : 1. 85m×0.2m) , shown as Figs. 5 and 7. In this version, profiles of jet stream near the fans could not be calculated adequately yet, then the flow was caused by setting appropriate values of pressure differences at both ends. The physical calculation time step was 0.1 second. The depth and the length of the layers are considered as one of the important parameters in this model, however they are not as sensitive as the mesh size in CFD models. Here they were adjusted to the points of the thermocouples in the experiment.

For reference the calculation results of the same conditions by FDS ver.4 (NIST) were added on each graph. The number of meshes was about 500,000. However, the heat release rate from the same size of the fuel pan with the experiment was much larger. The main reason is that in the model the fuel was heated more by radiation from the flame and evaporated more, whereas in the tests the fuel was cooled by the water outside the fuel pan. Therefore the size was set to be almost a half to adjust to the same heat release rate of the experiment. For the jet fans, objects of almost the same size and location were created and set to flow in at one side and out at the other side.

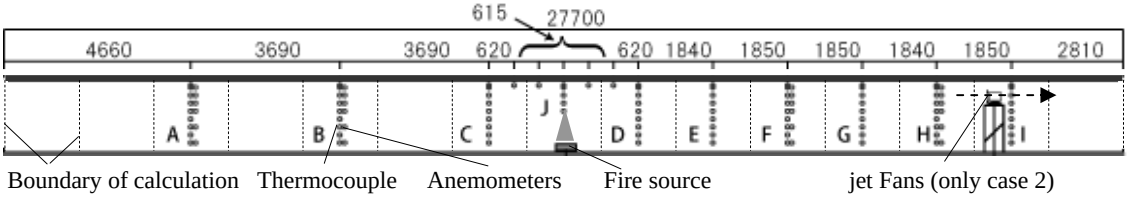

Fig. 5 Longitudinal section of the facility and division of area

Fig. 6. Inside of the facility

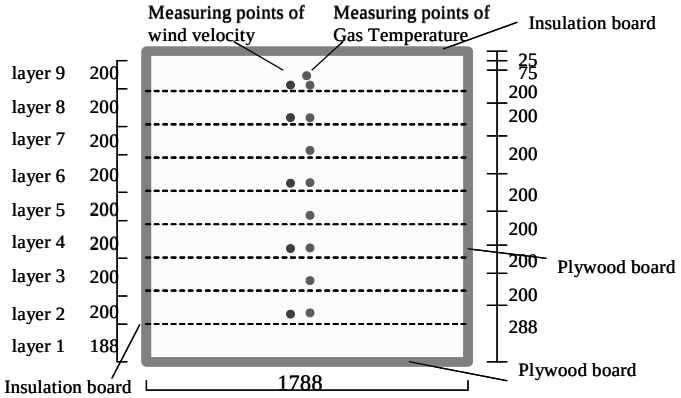

Fig. 7. Cross section of the facility and division of layer

Computer Time

The CPU time of the calculation by the MLZ model was within 100 seconds for computing 150 seconds by a PC (with Pentium4, 3.06 GHz). In the other hand, the CPU time by FDS was 25 hours for the same problem. Hence it could be found that MLZ model has the much advantage of using less computing time.

Analysis

Figure 8 shows the comparisons with the experiment and two calculation results of the vertical distribution of temperature at 150 second (at almost steady-state) for Case 1 (natural ventilation condition). The results by the MLZ model were in good agreement with the experiment, except for heights ranging from 0.7 to

1.1m. However, this difference is small and on the conservative side for design problems. On the contrary, the calculation result by FDS was lower within the height ranging from 1.1 to 1.5m. Fig.10 shows the results for case 2 (mechanical ventilation of 0.5m/s). The result by MLZ agreed well at downstream locations, lines D (+5.5m) and F (9.2m). However, the agreement was not good in the upwind side, line B (-5.5m). It seems that the MLZ model underestimated the back layering. The results by FDS were overall higher at height more than 1.1m. Fig.12 shows the distribution image of the gas temperature predicted by MLZ . The numbers on the figure show the gas temperature values [°C], and the density of black and white is proportional to it.

Figure 9 shows the comparisons of the vertical distribution of the velocity at 150 second (as almost steady-state) for Case 1 (natural ventilation). The results by MLZ were a little higher at 1.7m. The results by FDS were much closer than the results of MLZ. Fig.11 shows velocities for Case 2 (mechanical ventilation of 0.5m/s). The results by MLZ are lower at 1.5 and 1.7m.

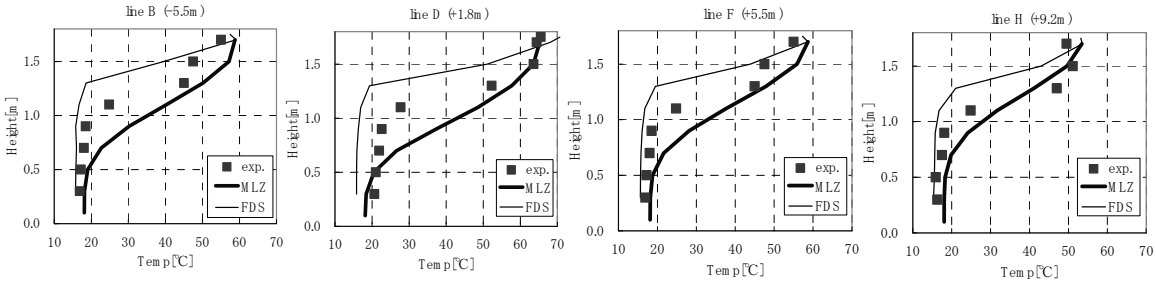

Fig. 8. Comparison of experiment and calculation for gas temperature (case 1, natural ventilation)

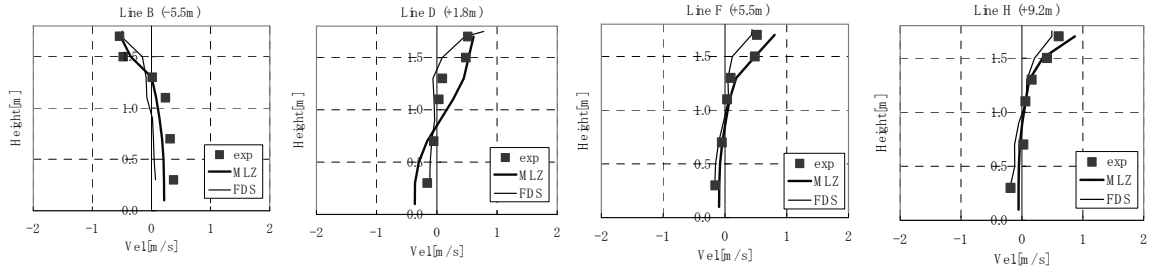

Fig. 9. Comparison of experiment and calculation for velocity (case 1, natural ventilation)

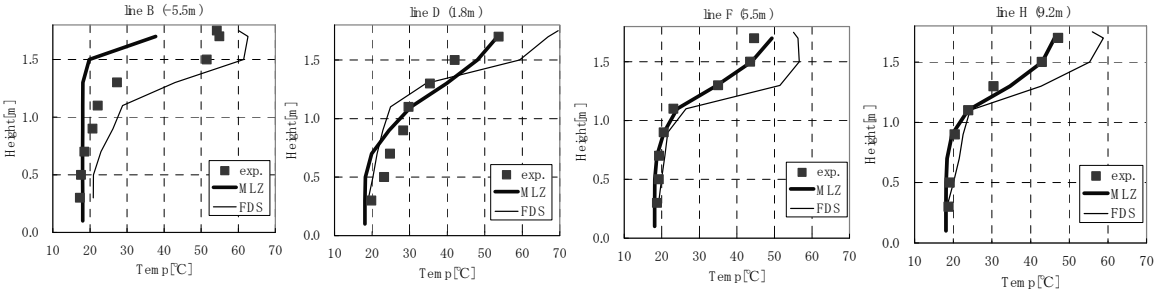

Fig. 10. Comparison of experiment and calculation for gas temperature (case 2, 0.5m/s)

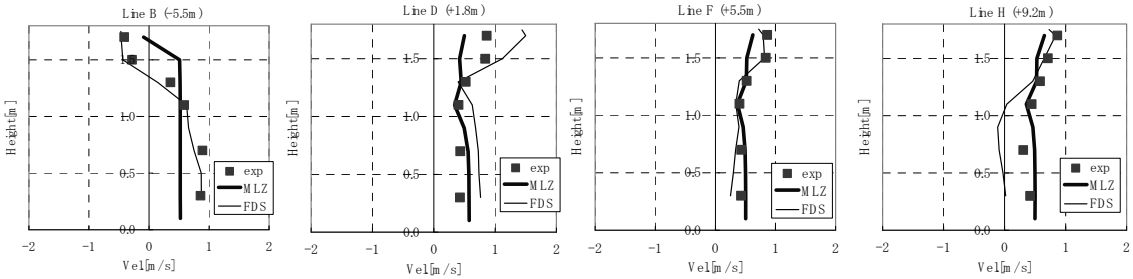

Fig. 11. Comparison of experiment and calculation for velocity (case 2, 0.5m/s)

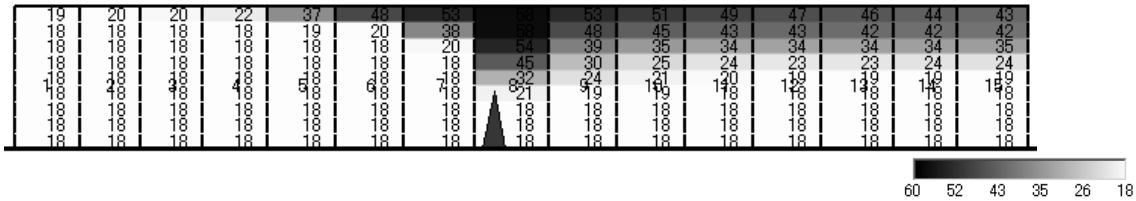

Fig. 12. Calculation result of gas temperature by MLZ (case 2, 0.5m/s) [°C]

CONCLUSION

- In this study, the concept and mathematical formulation of a Multi Layer Zone (MLZ) model were introduced as one of the prominent tool for tunnel fire safety designs.
- The model provides comparatively detailed and accurate temperature distributions and the calculation speed is much faster than that of CFD simulations.
- Except for back layering, the predicted temperature and velocity results generally show good agreement with the experiments. Especially some of the temperature results were much closer than the FDS predictions.

REFERENCES

[1] Kumar, S., “Field Model Simulation of Vehicle Fires in a channel Tunnel Shuttle Wagon ”, the 4-th Symposium of IAFSS, 1992. doi:10.3801/IAFSS.FSS.4-995

[2] Tanaka, T. and Nakamura, K., “A Model for Predicting Smoke Transport in Buildings -Base on Two Layer Zone Concept –”, Building Research Institute, No.123, BRI, MOC, 1989.

[3] Charters, David A., Gray, W. Alan, McIntosh, Andrew C., “A Computer Model to Assess Fire Hazards in Tunnels (FASIT)”, Fire Technology First Quarter, 1994.

[4] Suzuki, K., Harada K., and Tanaka, T., “A Multi-Layer Zone Model for Predicting Fire Behavior in a Single room”, the 6-th Symposium of IAFSS, Jun. 2001.

[5] Delichatsios, M.A., “Air entrainment into buoyant jet flames and pool fires”, *The SFPE Handbook of Fire Protection Engineering (2nd ed),* DiNenno P.J. (ed.), National Fire Protection Association, Quincy, MA 02269, 1995, p. **2**-20

[6] Quintiere, J.G. et al., The Effect of Room Openings on Fire Plume Entrainment, Combustion Science and Technology, 1981.

[7] Modak, A.T., “Radiation from products of Combustion”, Fire Research, 1, 1978/79Davis, W.D. and Reneke, P., “Predicting Smoke Concentration in the Ceiling Jet,” National Institute of Standards and Technology Report NISTIR 6480, Gaithersburg, MD, 2000, 12 p.